Available online at www.sciencedirect.com
SCIENCE DIRECT
Coastal Engineering 53 (2006) 99 – 113
Coastal Engineering
An International Journal for Coastal, Harbour and Offshore Engineers
www.elsevier.com/locate/coastaleng

Experimental study on the hydrodynamics of regular breaking waves

Francesca De Serio [a,1], Michele Mossa [b,*]

[a] DIAC, Technical University of Bari, Via E. Orabona, 4-70125 Bari, Italy
[b] DIASS, Technical University of Bari, Via E. Orabona, 4-70125 Bari, Italy

Received 2 December 2004; received in revised form 25 May 2005; accepted 14 September 2005
Available online 28 November 2005

Abstract

This paper illustrates the results of experimental research carried out in the wave flume of the Water Engineering and Chemistry Department laboratory of Bari Technical University (Italy) and based on the analysis of three different regular waves breaking on a sloping bottom. The investigation refers particularly to the surf zone, with the aim to develop two themes: the study of velocity and Reynolds shear stress distributions in the shoaling zone of a regular wave field and the study of turbulence in the breaking region, observing that these two aspects greatly influence many coastal processes, such as undertow currents, sediment transport and action on maritime structures.

Keywords: Regular waves; Shear stress; Turbulence; Kinetic energy

1. Introduction

The vertical flow structure in the surf zone is a subject of great importance in coastal engineering in order to understand many correlated processes. The velocity distribution of longshore currents and undertow, the sediment concentration field, the wave set-up and the wave-driven currents in the surf zone are all phenomena which depend on the flow field in breaking waves (Christensen and Deigaard, 2001). Moreover, surf zone dynamics hold a pivotal role in the dynamic equilibrium of beaches because it can be considered a seaward boundary of the swash zone, that is, the region of shoreline erosion and accretion (Elfrink and Baldock, 2002; Longo et al., 2002). Since the first pioneering work (see Stive, 1980), it has been evident that the study of turbulent flow mechanisms in breaking waves has represented a difficult task for many researchers due to the extreme unsteadiness and non-uniformities associated with it. In fact, wave breaking is characterized by a sudden transition from irrotational to rotational motion with a violent transformation of wave energy into turbulence and eventually into heat (Feng and Stansby, 2002; Pedersen et al., 1998).

In the horizontal direction of the surf zone, the following zones can be distinguished (Christensen et al., 2002). Initial wave deformation occurs in what has been termed the shoaling zone, where wave profile is characterized by a rapid change in shape. Subsequently, the wave reaches the breaking point in the outer zone, originating from an overturning jet, whose strength depends on the type of breaker. In the inner surf zone, the wave undergoes a gradual transformation into a turbulent bore, until reaching the swash zone.

It is the shoaling and outer zones that are of interest to this paper, which focuses on spilling, plunging and spilling/plunging breakers (i.e., the intermediate range between spilling and plunging, taking into account the Irribarren number). Firstly, the investigation analyses velocity and Reynolds shear stress distributions of the regular wave field on a sloping bottom, and successively, it deals with the study of turbulence in the region where breaking occurs (De Serio and Mossa, 2003a,b).

Referring to the first part of the research, it must be pointed out that the following question has arisen in some recent literature (Rivero and S.-Arcilla, 1995; Deigaard and Fredsøe, 1989; Svendsen, 1984). For real waves propagating over a sloping bottom and with energy dissipation, the phase shift between horizontal and vertical components of the wave motion is different from $\pi/2$, i.e., the value predicted by classical theories. Consequently, those wave-induced circulation models

* Corresponding author. Tel.: +39 80 596 3289; fax: +39 80 596 3414.
E-mail addresses: f.deserio@poliba.it (F. De Serio), m.mossa@poliba.it (M. Mossa).
[1] Tel.: +39 80 596 3557; fax: +39 80 596 3414.

0378-3839/$ - see front matter © 2005 Elsevier B.V. All rights reserved.
doi:10.1016/j.coastaleng.2005.09.021

which neglect the shear stress contribution in the momentum balance equations demonstrate inconsistencies in their results. In order to solve this problem and to evaluate the vertical wave Reynolds shear stress distribution, some formulations have been developed by Rivero and S.-Arcilla (1995), Deigaard and Fredsøe (1989), and You (1997) in the case of both irrotational and rotational wave motion. As observed by You (1997), Rivero and S.-Arcilla (1997), and Damiani and Mossa (1999), the aforementioned formulations do not always coincide, so they need further confirmation on the basis of laboratory tests. For example, the time-averaged cross-correlation between $\tilde{u}$ and $\tilde{w}$, i.e., $\overline{\tilde{u}\tilde{w}}$, has been discussed by Rivero and S.-Arcilla (1995) and by You (1997), who were not in agreement on the results.

Therefore, it is important to highlight that some of the questions discussed in this paper are still open, even if already discussed in literature. On this point, Ting and Kirby (1996) wrote that "turbulence transport processes are different in spilling and plunging breakers" and suggested "that further work on this topic is warranted." The first aim of this work is to provide data on the spatial correlation in the vertical direction and to contribute to the validation of the aforementioned models.

The second part of the present study springs from the necessity for predictive models of coastal processes to correctly explain the spatial and temporal variations of turbulence in the surf zone and the correlation between the flow and the turbulence level in order to qualitatively explain cross-shore sediment transport mechanisms (Ting and Kirby, 1994, 1995, 1996).

It should be noted that in the present work of the evaluation of organised and turbulent fluxes, the turbulent kinetic energy is directly obtained by experimental results and, consequently, no doubt persists about their signs and trends. On the contrary, previous researchers (Ting and Kirby, 1995, 1996) based their considerations on the transport of turbulent kinetic energy by turbulent velocity fluctuations $\langle u'k'\rangle$ and $\langle w'k'\rangle$ by evaluating the diagram of some terms which contribute to $\langle u'k'\rangle$ and $\langle w'k'\rangle$, respectively, arguing that the sign of these terms presumably followed the sign of these fluxes.

The investigation has been carried out in the wave flume of the Water Engineering and Chemistry Department laboratory of Bari Technical University (Italy) and it is based on the analysis of three regular waves with different characteristics.

The governing equations of the problem are described in Section 2. Section 3 illustrates the adopted experimental set-up and procedure. The experimental results are presented and discussed in Section 4 regarding velocities and shear stress distributions, while Section 5 deals with the analysis of turbulence parameters.

2. Theoretical background

The problem is governed by the Navier–Stokes equations and for simplicity is confined to a 2D frame, in which the waves propagate along the x direction and the z axis is directed vertically upward from the free surface. Taking into account that any physical quantity can be split into the steady mean flow component, i.e., time-averaged component (indicated by capital letters or the over-bar), the fluctuation component due to the statistical contribution of the wave (indicated by the tilde symbol) and the fluctuation component of the turbulence (indicated by the prime symbol) the velocity component u_i ($i=1,2$) can be expressed as follows:

$$u_i(x_i,t) = \langle u_i\rangle(x_i,t) + u'_i(x_i,t) = U_i(x_i) + \tilde{u}_i(x_i,t) + u'_i(x_i,t) \quad (1)$$

where t is the time quantity, x_1 and x_2 are, respectively, the x and z Cartesian coordinates and the angular brackets $\langle\rangle$ are an operator to take an ensemble average. Ensemble averaging requires the phenomenon to be highly reproducible, i.e., repeatable conditions and a sufficiently large number of repetitions to obtain stable statistical values. The method is vulnerable to small displacements in time and space of the mean properties, which can easily occur for broken waves (Longo et al., 2002). In the present study, where regular waves are analysed, the ensemble average method can be adopted (Okaiasu et al., 1986; Feng and Stansby, 2002) by phase-averaging the measured signals over a great number of cycles. Then, these values were averaged to yield the time-averaged velocities. Consequently, turbulent fluctuations were obtained as the difference between the original time series and the ensemble-averaged velocities.

Using the Cartesian tensor notation, the ensemble-averaged motion equations of the incompressible fluid are:

$$\frac{\partial\langle u_i\rangle}{\partial t} + \frac{\partial\langle u_i\rangle\langle u_j\rangle}{\partial x_j} = \frac{1}{\rho}\frac{\partial}{\partial x_j} \times \left(-\langle p\rangle\delta_{ij} + 2\mu\frac{1}{2}\left(\frac{\partial\langle u_i\rangle}{\partial x_j} + \frac{\partial\langle u_j\rangle}{\partial x_j}\right) - \rho\langle u'_i u'_j\rangle\right) \quad (2)$$

where ρ is the water density, δ_{ij} is the Kronecker delta, p is the hydrodynamic pressure, and μ is the dynamic viscosity.

The motion is periodic, so the average over the period T of Eq. (2), by using Eq. (1) and the continuity equation, becomes

$$\frac{\partial}{\partial x_j}\left(U_iU_j + \overline{\tilde{u}_i\tilde{u}_j} + \overline{u'_iu'_j}\right) = \frac{1}{\rho}\left(-\frac{\partial P}{\partial x_j}\delta_{ij} + \mu\frac{\partial^2 U_i}{\partial x_j\partial x_j}\right). \quad (3)$$

The cross products $\overline{\tilde{u}_i\tilde{u}_j}$ and $\overline{u'_iu'_j}$ appearing in Eq. (3) are, respectively, the wave Reynolds stresses and the turbulent Reynolds stresses, apart from the contribution of the water density ($-\rho$).

Rivero and S.-Arcilla (1995) derived theoretically that the vertical distribution of the wave Reynolds shear stresses in the following cases by relating it to the vorticity of the oscillatory flow: irrotational non-dissipative flow on a sloping bottom (observing that they are nil only in the case of irrotational non-dissipative flow on a horizontal bottom); irrotational dissipative flow; and rotational flow.

Observing that surf zone turbulence originates from instabilities of surface waves, the fundamental source of energy

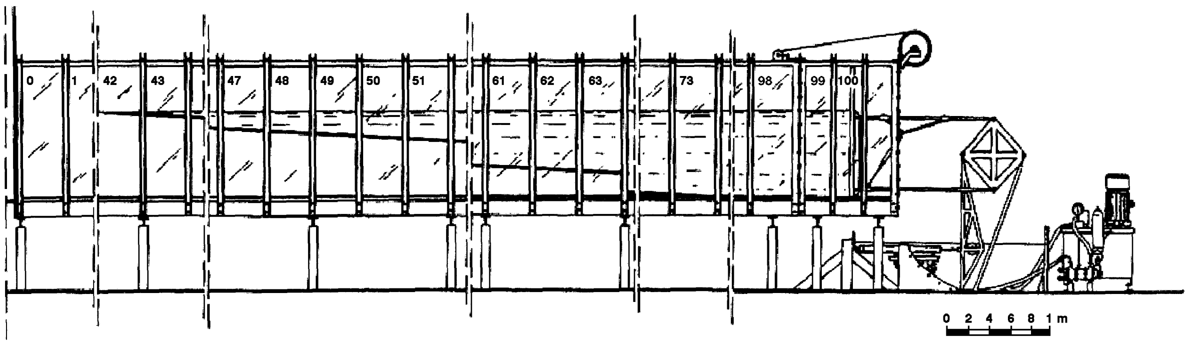

Fig. 1. Sketch of the wave flume.

for turbulence is the kinetic energy, released by breaking, whose ensemble average is defined as:

$$k = \frac{1}{2}\langle u'_i u'_i \rangle. \tag{4}$$

The distribution of k may be determined by solving the equation of conservation of the turbulent kinetic energy (Damiani and Mossa, 1999), which states that the local time rate change of turbulent kinetic energy is due to convection by mean flow, diffusive transport by pressure and turbulent fluctuations, turbulent energy production and viscous dissipation:

$$\frac{\partial}{\partial t} + \frac{\partial \langle u_j \rangle k}{\partial x_j} = \frac{\partial}{\partial x_j}\left(\frac{1}{\rho}\langle u'_j p' \rangle + \langle u'_j k' \rangle - 2\nu \langle u'_j s'_{ij} \rangle\right) - \langle u'_i u'_j \rangle \frac{1}{2}\left(\frac{\partial \langle u_i \rangle}{\partial x_j} + \frac{\partial \langle u_j \rangle}{\partial x_i}\right) - 2\nu \langle s'_{ij} s'_{ij} \rangle \tag{5}$$

with

$$k' = \frac{1}{2} u'_i u'_i \tag{6}$$

$$s'_{ij} = \frac{1}{2}\left(\frac{\partial u'_i}{\partial x_j} + \frac{\partial u'_j}{\partial x_i}\right) \tag{7}$$

and p is the hydrodynamic pressure.

The determination of k is fundamental to evaluate the turbulent diffusion coefficient and, consequently, the turbulent mass transport (assumed to be related to the gradient of the transported quantity, on the analogy of turbulent momentum transport).

As observed by Ting and Kirby (1995, 1996) experimental confirmation is required for the hypothesis that the main production phase of turbulent kinetic energy takes place above the trough level, while the spreading of turbulent energy is primarily due to convection.

A consideration must be pointed out. In the experiments by Ting and Kirby (1996), the horizontal and vertical components of water particle velocity were not measured at the same time, but by conducting the same experiment twice. In particular, because of this technical limitation, the value and sign of some quantities could not be directly evaluated by referring to the historical series of the acquired signal, but they could be evaluated only by calculating some of their component terms.

On the contrary, in the present research, horizontal and vertical velocities were assessed simultaneously. This possibility allowed us to examine fluxes and correlation coefficients directly.

3. Experimental equipment and procedure

The 45-m-long and 1-m-wide wave channel used to carry out the tests is located in the Water Engineering and Chemistry Department laboratory of Bari Technical University (Italy). The iron frames supporting its crystal walls are numbered from the shoreline up to the wavemaker (section 100), thus locating measurement sections which have a center to center distance

Table 1
Principal characteristics of the examined regular waves

Section	d [cm]	H [cm]	T [s]	L_A [m]	U	Zone
Test 1						
63	47.0	12.1	2.0	3.95	18	Shoaling
55	31.0	12.4	2.0	3.31	46	Shoaling
51	21.0	15.5	2.0	2.77	2	Shoaling
49	16.5	14.3	2.0	2.47	194	Shoaling
48	14.0	11.7	2.0	2.29	2	Outer
47	11.3	5.9	2.0	2.06	174	Outer
46	10.0	5.6	2.0	1.95	213	Inner
45	8.5	4.9	2.0	1.80	259	Inner
Test 2						
63	47.0	7.5	1.0	1.50	2	Shoaling
55	31.0	7.1	1.0	1.38	5	Shoaling
51	21.0	7.2	1.0	1.23	2	Shoaling
49	16.5	7.7	1.0	1.13	2	Shoaling
48	14.0	7.3	1.0	1.06	0	Outer
47	11.3	7.1	1.0	0.97	46	Outer
46	10.0	5.1	1.0	0.92	43	Outer/inner
45	8.5	4.6	1.0	0.86	55	Inner
Test 3						
63	47.0	6.7	4.0	8.42	6	Shoaling
55	31.0	8.1	4.0	6.88	129	Shoaling
51	21.0	10.6	4.0	5.69	1	Shoaling
49	16.5	11.2	4.0	5.05	636	shoaling
48	14.0	12.9	4.0	4.66	21	Outer
48′[a]	13.0	11.5	4.0	4.49	55	Outer
47	11.3	9.2	4.0	4.19	1119	Outer
46	10.0	7.2	4.0	3.95	23	Outer/inner
45	8.5	5.8	4.0	3.64	51	Inner

[a] In the intermediate distance between sections 47 and 48.

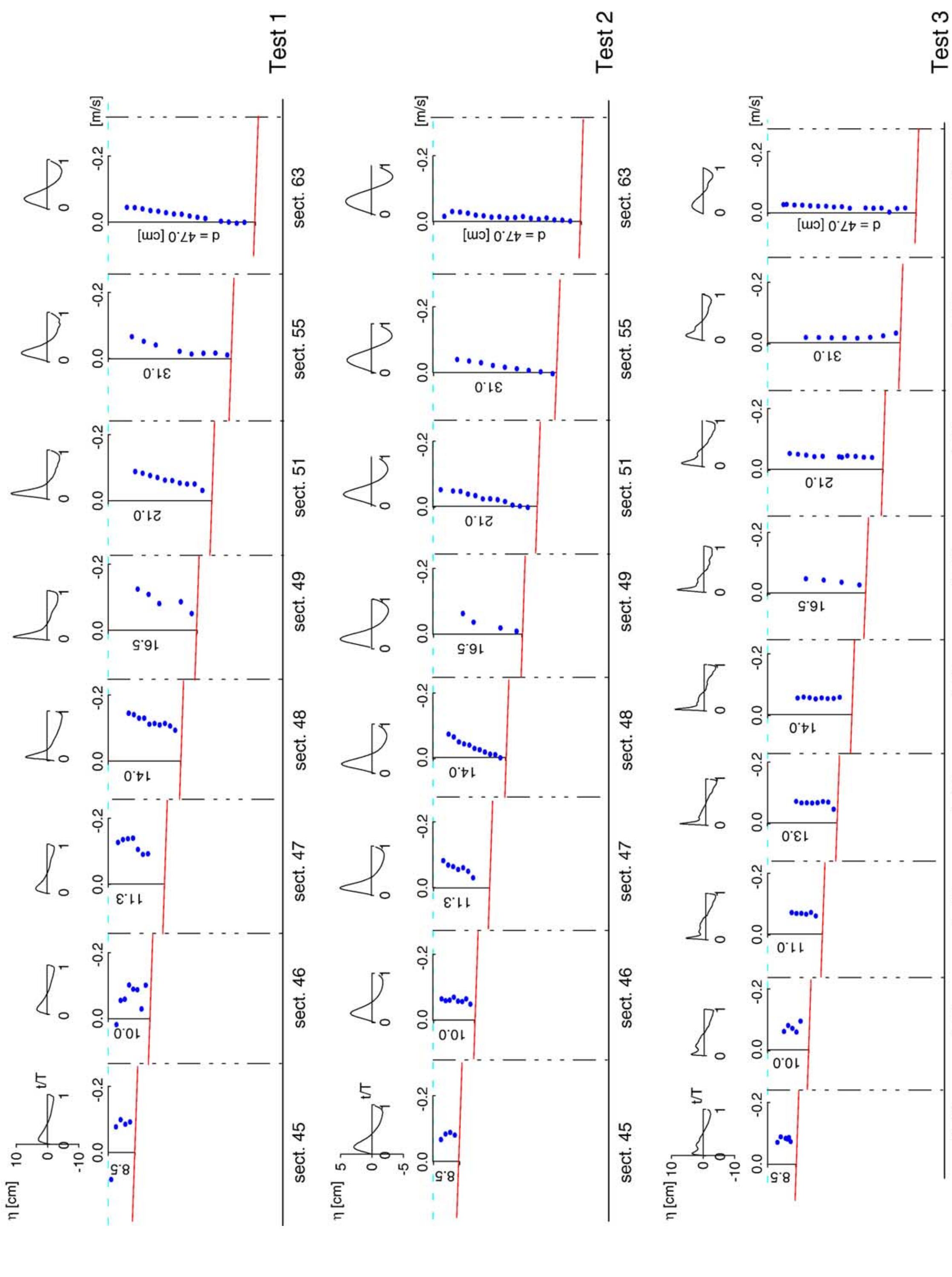

Fig. 2. Time-averaged horizontal velocity component $\bar{u}$.

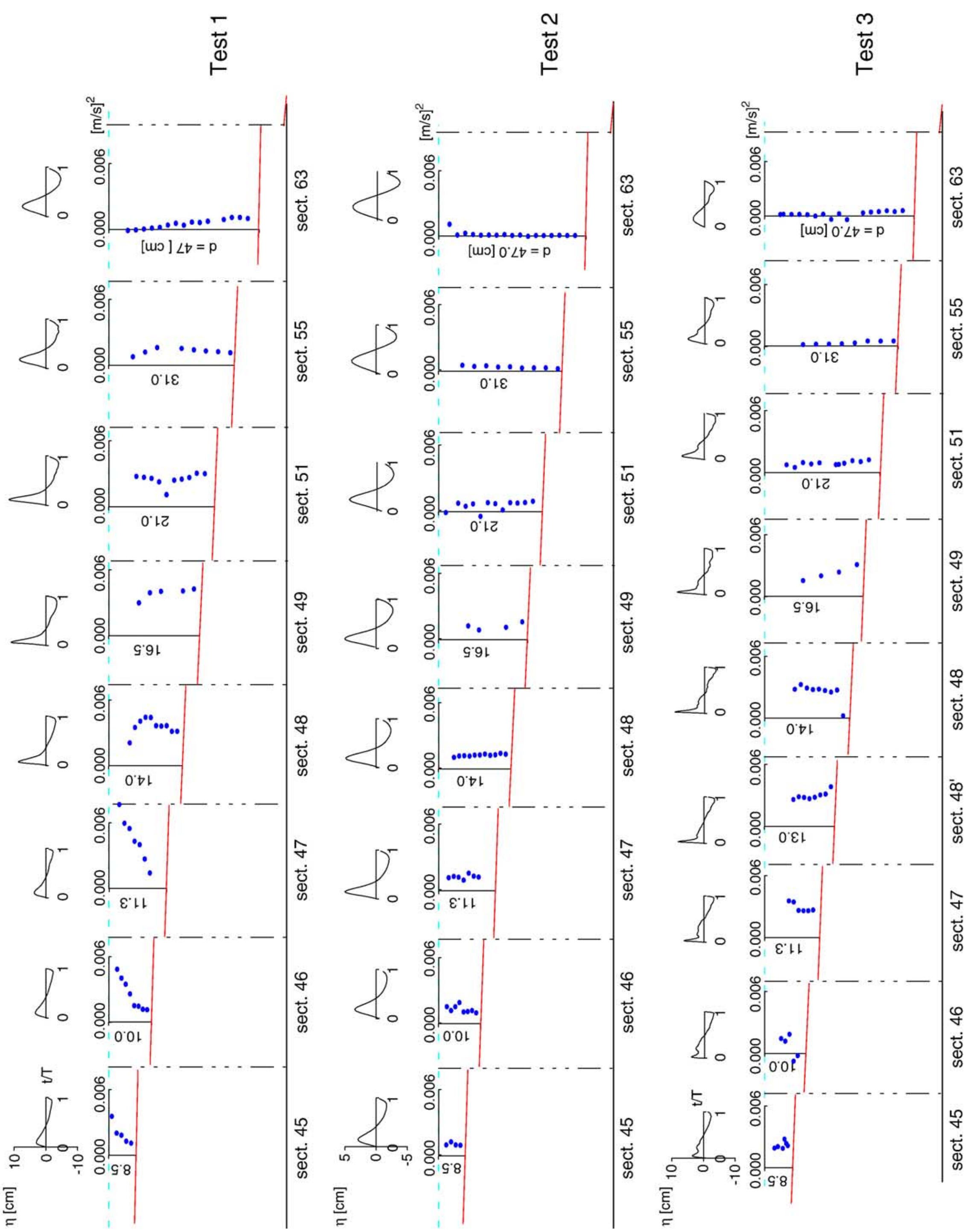

Fig. 3. Vertical distribution of the correlations $\overline{\tilde{u}\tilde{w}}$.

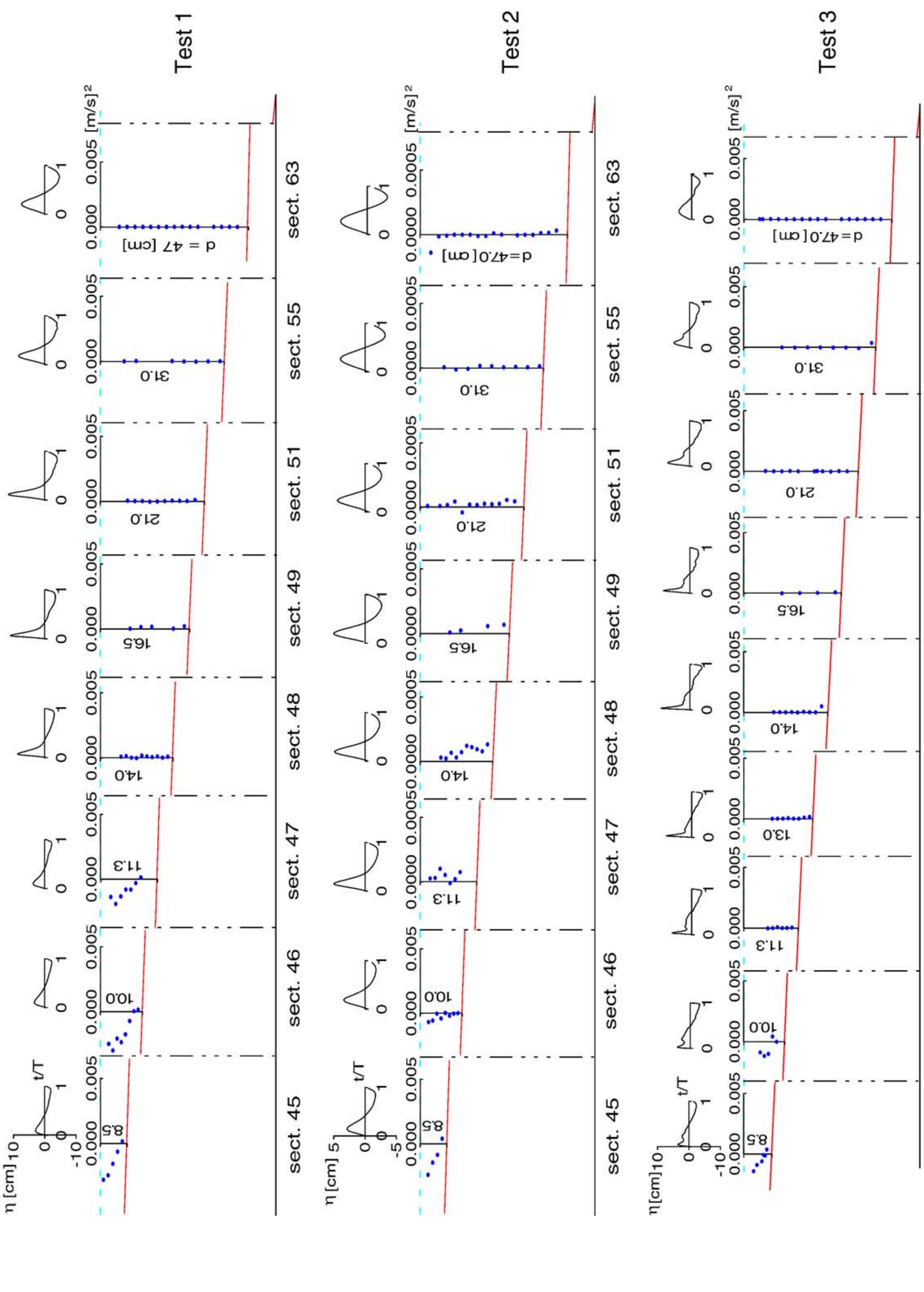

Fig. 4. Vertical distribution of the correlation $\overline{uw}$.

equal to 0.44 m. From the wave paddle to section 73, the flume has a flat bottom, while from section 73 up to the shoreline, it has a 1/20 sloped wooden bottom. A sketch of the wave flume is shown in Fig. 1.

Table 1 shows the main characteristics of the tested regular waves, evaluated in the different sections, where d is the mean water depth, H and T the wave height and period, L_A the wave length according to the Airy theory, $U=HL_A^2/d^3$ the Ursell number, indicator of a non-linear wave behaviour.

Taking into account the Irribarren breaking number ξ_b, the wave fields of the present study are characterized, respectively, by a spilling/plunging breaker in test 1 ($\xi_b=0.37$), a spilling breaker in test 2 ($\xi_b=0.23$) and a plunging breaker in test 3 ($\xi_b=0.74$). The offshore steepness of the plunging breaker chosen was much smaller than that of the spilling breaker, so for a typical sediment fall velocity, the spilling and plunging breakers could be classified as erosional and accretional waves, respectively (Ting and Kirby, 1994).

Like most of the recent experimental investigations (Okaiasu et al., 1986; Feng and Stansby, 2002), the Laser Doppler Anemometry, a modern non-intrusive measurement technique, was used to measure the instantaneous Eulerian velocity. In particular, a backscatter, two-component four-beam

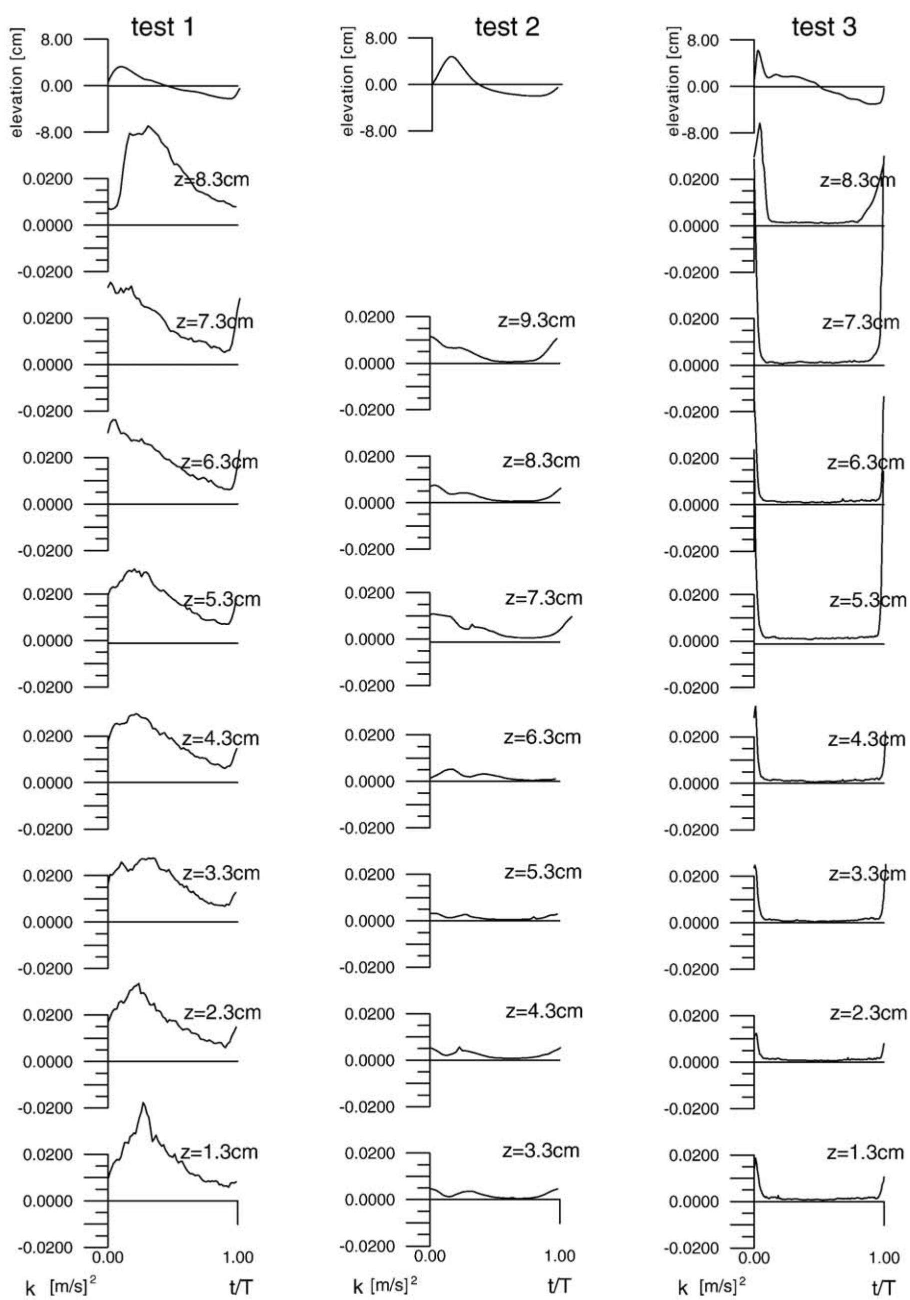

Fig. 5. Diagram of k during one wave period at the investigated depth in section 47, referring, respectively, to test 1 (spilling/plunging), test 2 (spilling) and test 3 (plunging).

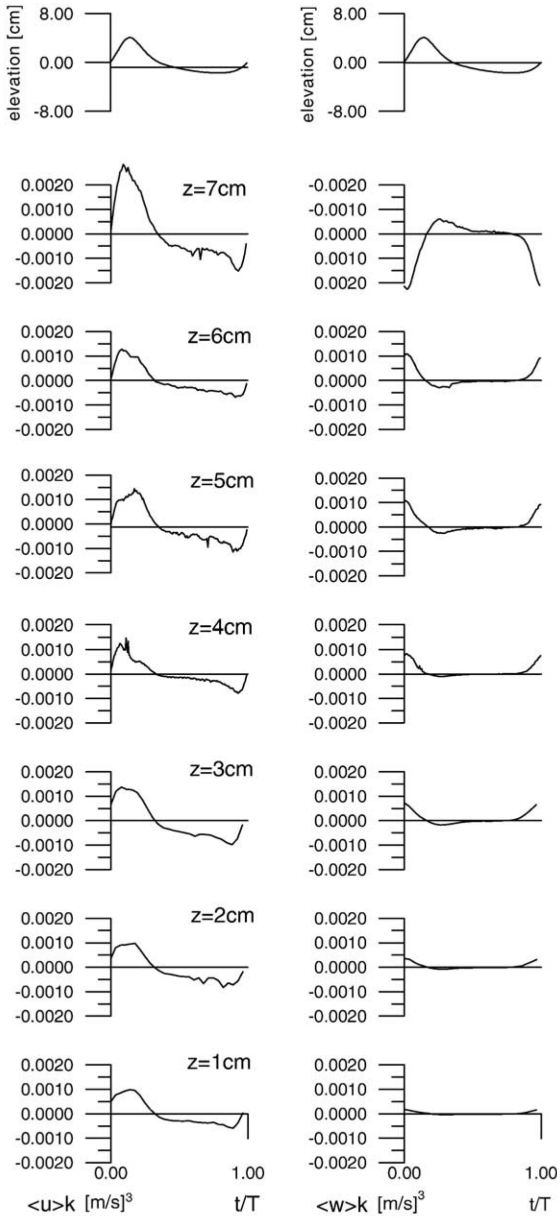

Fig. 6. Diagram of $\langle u\rangle k$ and $\langle w\rangle k$ during one wave period at the investigated depths in section 46. Results of test 2.

LDA system and a Dantec LDA signal processor (58N40 FVA Enhanced) based on the covariance technique (Damiani and Mossa, 1999) was adopted. The wave elevations were measured with a resistance probe placed in the transversal section of the channel crossing the laser measuring volume. The velocity and wave elevation measurements were assessed simultaneously, allowing us to perform the phase-averaging analysis. The velocity components measured in the present study are u in the x direction, conventionally established as positive if oriented onshore, and w in the vertical direction, conventionally established as positive if oriented upward. All the velocity measurements were assessed in many vertical sections between the bottom boundary layer and the wave trough, i.e., in the middle region of surf-zone, due to the fact that LDA suffers from signal drop-out within the aerated region.

4. Analysis of velocity field and shear stresses distributions

Fig. 2 shows the vertical distributions along the channel of the time-averaged horizontal velocity components for all the three tests. For each investigated section, the wave elevations η are sketched above the $\bar{u}$ profile. From Fig. 2, it is possible to observe that for most measurement points the values are negative, i.e., offshore directed, while, confirming the mass continuity, they become positive, i.e., onshore directed, near the bottom (see sections 51 and 55 of test 2), and in the trough-crest region. As expected, the horizontal mean velocities are small in the offshore sections (section 63), where the wave behaviour is similar to the linear one, while near the breaking region, they increase, giving rise to the strong undertow current. Moreover, it is observed that in all the tests, the $\bar{u}$ vertical profiles show values close to zero near the bed with an increasing trend of their absolute values from the bottom to the free surface. The vertical profiles of Fig. 2 have a triangular shape for tests 1 and

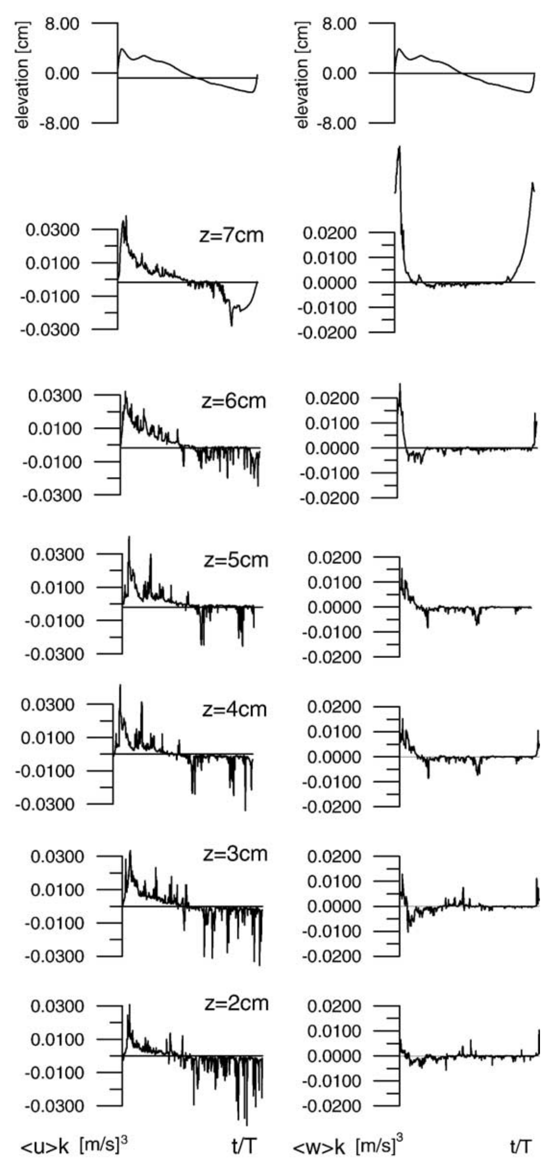

Fig. 7. Diagram of $\langle u'k'\rangle$ and $\langle w'k'\rangle$ during one wave period at the investigated depths in section 46. Results of test 3.

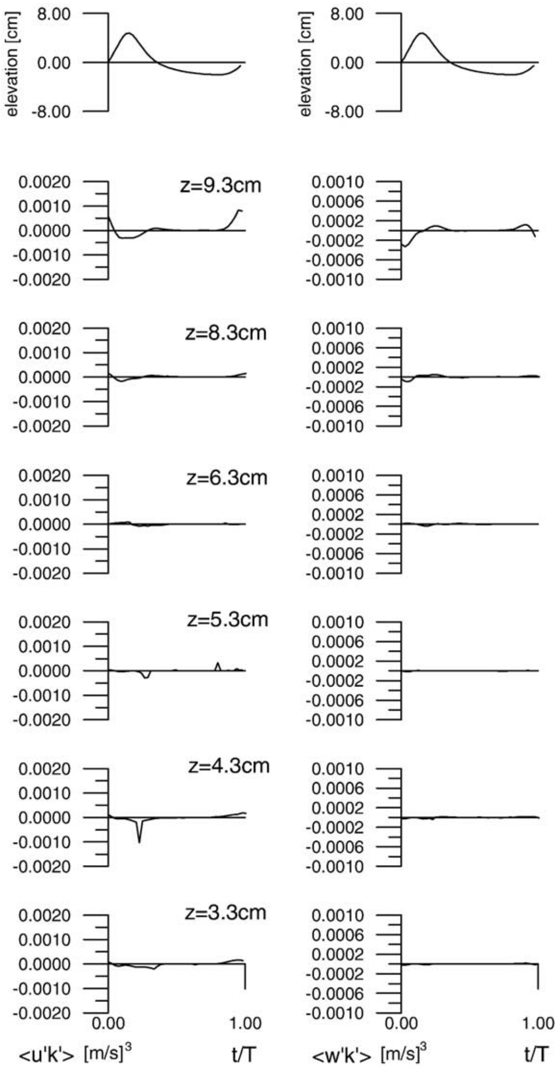

Fig. 8. Diagram of $\langle u\rangle k$ and $\langle w\rangle k$ during one wave period at the investigated depths in section 47. Results of test 2.

2, except for the breaking sections, while for test 3, they are quite flat along the vertical sections, due to the stronger turbulent effects typical of a plunging breaking. The mean values of the vertical velocity components, generally smaller than those of the horizontal ones, are not shown in the present paper for the sake of brevity.

The experimental data highlight a phase shift between $\tilde{u}$ and $\tilde{w}$ different from $\pi/2$ at each investigated depth, confirming the observations of Gudmestad and Connor (1980) and Rivero and S.-Arcilla (1995). Fig. 3 shows the vertical distributions of the correlations $\overline{\tilde{u}\tilde{w}}$ (i.e., wave Reynolds shear stresses, apart from the water density $-\rho$) for all the measurement points. Again, the phase-averaged wave surface profiles are sketched above each section.

For all the tests, it is clear that in the sections offshore the breaking region, the vertical trend of $\overline{\tilde{u}\tilde{w}}$ is quite linear, generally decreasing with distance from the bottom. Taking into account the convention of the velocity signs, the maximum positive values are located near the bed; on the contrary, negative values are present in the points closer to the wave trough. These results are in agreement with those of Rivero and S.-Arcilla (1995, 1997). In fact, both the sign (positive) and the trend (decreasing upwards) of the vertical distribution of $\overline{\tilde{u}\tilde{w}}$ is correctly predicted by the authors' model. Approaching the breaking region (sections 49 and 48 of test 1 and test 2, and sections 49, 48 and 48′ of test 3), it is possible to observe that $\overline{\tilde{u}\tilde{w}}$ is always positive. Also, the aforementioned results agree with the theoretical distributions proposed by Rivero and S.-Arcilla (1995) for the case of dissipative waves propagating over a sloping bottom. The theoretical model for dissipative waves over a sloping bottom proposed by Deigaard and Fredsøe (1989)

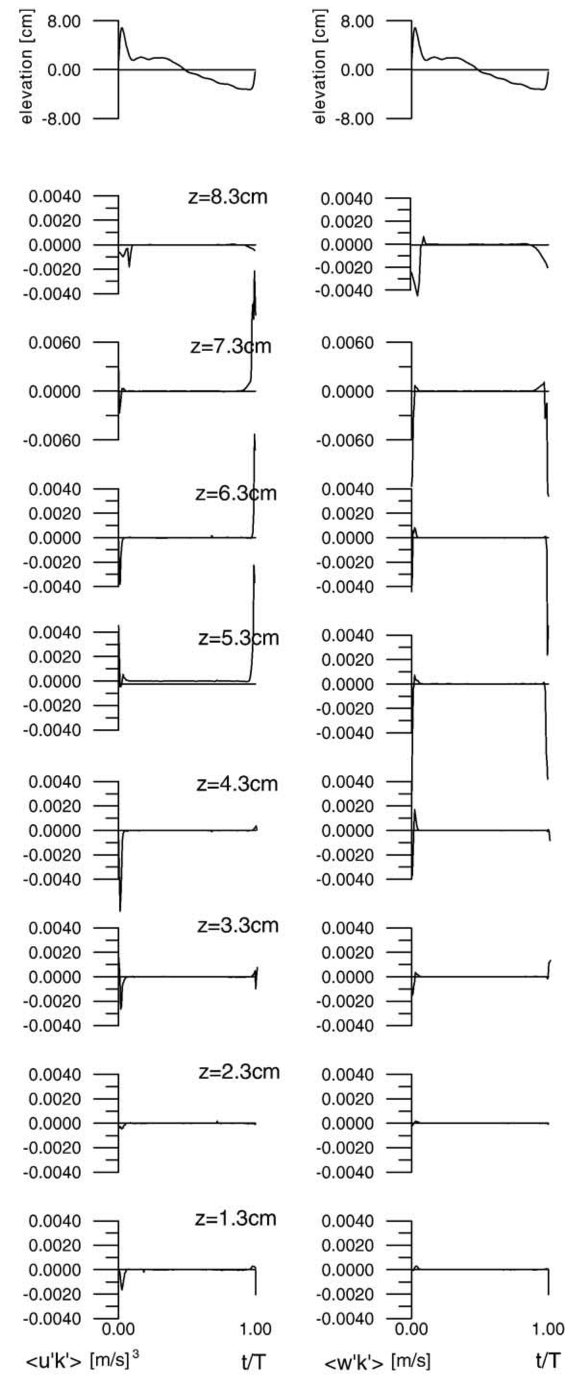

Fig. 9. Diagram of $\langle u'k'\rangle$ and $\langle w'k'\rangle$ during one wave period at the investigated depths in section 47. Results of test 3.

seems to be validated by $\overline{\tilde{u}\tilde{w}}$ trends in the outer and also in the inner breaking zone, where the vertical profile has an increasing trend from the bottom up to the free surface (see sections 47, 46 and 45 of test 1, sections 47 and 46 of test 2 and sections 47 and 46 of test 3).

Fig. 4 shows the vertical distributions of the turbulent velocity cross correlations $\overline{u'w'}$ (i.e., turbulent Reynolds shear stresses, apart from the water density $-\rho$). A comparison with the wave Reynolds shear stresses highlight that $\overline{u'w'}$ are generally smaller. Moreover, in the sections far away from the breaking region, the values of $\overline{u'w'}$ are always quite nil. They become greater only where the turbulence is not too weak, that is, only close to the breaking zone, showing a triangular trend with negative values for most measurement points.

5. Analysis of turbulence and turbulent transport

For the sake of brevity, the following results will be shown only for section 47, where there was wave breaking in all the three tests.

Fig. 5 shows the trend of k during one wave period at the investigated depths respectively in the case of spilling/plunging (test 1), spilling (test 2) and plunging (test 3) breaking. It must be noted that because the transverse velocity component was not measured, turbulent kinetic energy was estimated as $k=(1.33/2)(\langle u'^2\rangle+\langle w'^2\rangle)$ (Svendsen, 1987).

In all the three cases, it is observed that k and the wave elevation are quite in phase, with greater values under the crest. Whereas in test 1 the intensities of k do not vary appreciably along the vertical sections, in test 2 and particularly in test 3, values of k decrease downward, indicating that turbulent energy is dissipated while convecting from surface to bottom and it is spread by large-scale eddy motions.

In addition, Fig. 5 shows that turbulence intensity varies appreciably over the wave cycle, above all in the case of plunging breaking. In agreement with the results of Ting and Kirby (1995), it is higher under the wave front, showing a peak, and it decays rapidly after the wave crest passes. This aspect is indicative of a turbulence decay time that takes only a small fraction of the period to dissipate most of its energy because of the presence of macro vortices, thus confirming the conclusion of Ting and Kirby (1994) and Petti and Longo (2001). Indeed, for spilling and above all for spilling/plunging case, the decay time, referred to the wave period, is greater.

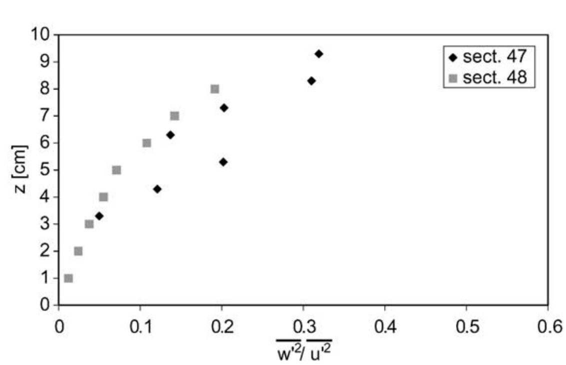

Fig. 10. Variation of w'^2/u'^2 in the spilling case.

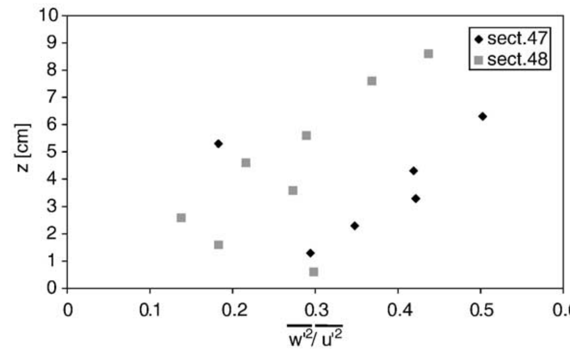

Fig. 11. Variation of w'^2/u'^2 in the plunging case.

Also, the partial temporal derivative of k, present in Eq. (5), shows an oscillating behaviour with a period equal to that of the wave. It is evident that $\partial k/\partial t$ vanishes when the wave elevation reaches its maximum and minimum values.

To give an example, the horizontal transport of turbulent kinetic energy by mean flow, $\langle u\rangle k$, and the vertical one, $\langle w\rangle k$, are shown in Fig. 6, referring to spilling breaker (test 2), and in Fig. 7, referring to plunging breaker (test 3). They are in reference to section 46, which is representative of the passage from outer to inner breaking for both spilling and plunging cases. The behaviour of spilling/plunging breaking is here not taken into consideration, having observed that it shows features which are intermediate between those of plunging and spilling breaking.

The analysis of Fig. 6 highlights that, in the spilling case, the energy flux by advection, $\langle u\rangle k$, is shoreward, under the wave front, and backward, under the trough, whereas the vertical energy flux, $\langle w\rangle k$, is upward under the crest. Moreover, at all depths, during the larger part of the wave period, $\langle u\rangle k$ is negative, and for most depths, the negative area of the diagram (i.e., the integral of the negative part of the function) prevails with respect to the positive area, thus stating that the horizontal turbulent transport is essentially directed offshore.

Fig. 7 highlights that under the crest of the plunging breaker, horizontal advection carries turbulent energy shoreward and vertical advection carries turbulent energy upward. In this case, analyzing the diagrams of $\langle u\rangle k$ at the different depths, the area under the positive curve results are greater than the negative one. This observation enables us to conclude that in the plunging breaking, the net turbulent transport is directed onshore. Consequently, taking into account that suspended sediment transport resembles turbulence transport $\langle u\rangle k$, it is possible to conclude that in the spilling breaker, the net sediment transport is offshore, while in the plunging breaker, it is directed onshore.

It must be underlined that in test 3 (plunging), the magnitude of $\langle u\rangle k$ is lightly stronger near the surface, indicating a greater turbulent transport in this region, while in test 2 (spilling), it lightly increases downward. These results show that the energy generated in the crest region is spread downward by moderate-scale eddies and it is transported offshore near the bottom.

Once the importance of integral properties which can provide information about local energy budget for different control volumes was realized, a depth-integrated horizontal flux of turbulent kinetic energy was calculated (Stive, 1980, 1985). For the most significant sections, the integral in depth of $\langle u \rangle k$ was derived. In the spilling case, the results underline that the turbulent kinetic energy flux spread away from the control volume offshore the outer zone, i.e., the volume between section 48 and section 49. Indeed, a storage of $\langle u \rangle k$ integrated in depth is evident in the volume between sections 46 and 47, in the transition zone from outer to inner zone. In the plunging case, on the contrary, the turbulent kinetic energy flux enters the volume between sections 47 and 48 immediately offshore the breaking zone, while it spreads away from the volume of breaking (sections 46–47).

The transport of k by turbulent velocity fluctuations is examined in Figs. 8 and 9 for test 2 and test 3, respectively, referring to section 47. In the case of spilling breaking, Fig. 8 shows, under the wave crest, maximum positive values of $\langle u'k' \rangle$and minimum negative values of $\langle w'k' \rangle$. Moreover, the transport of turbulent kinetic energy by turbulent velocity components seems essentially directed shoreward and down-

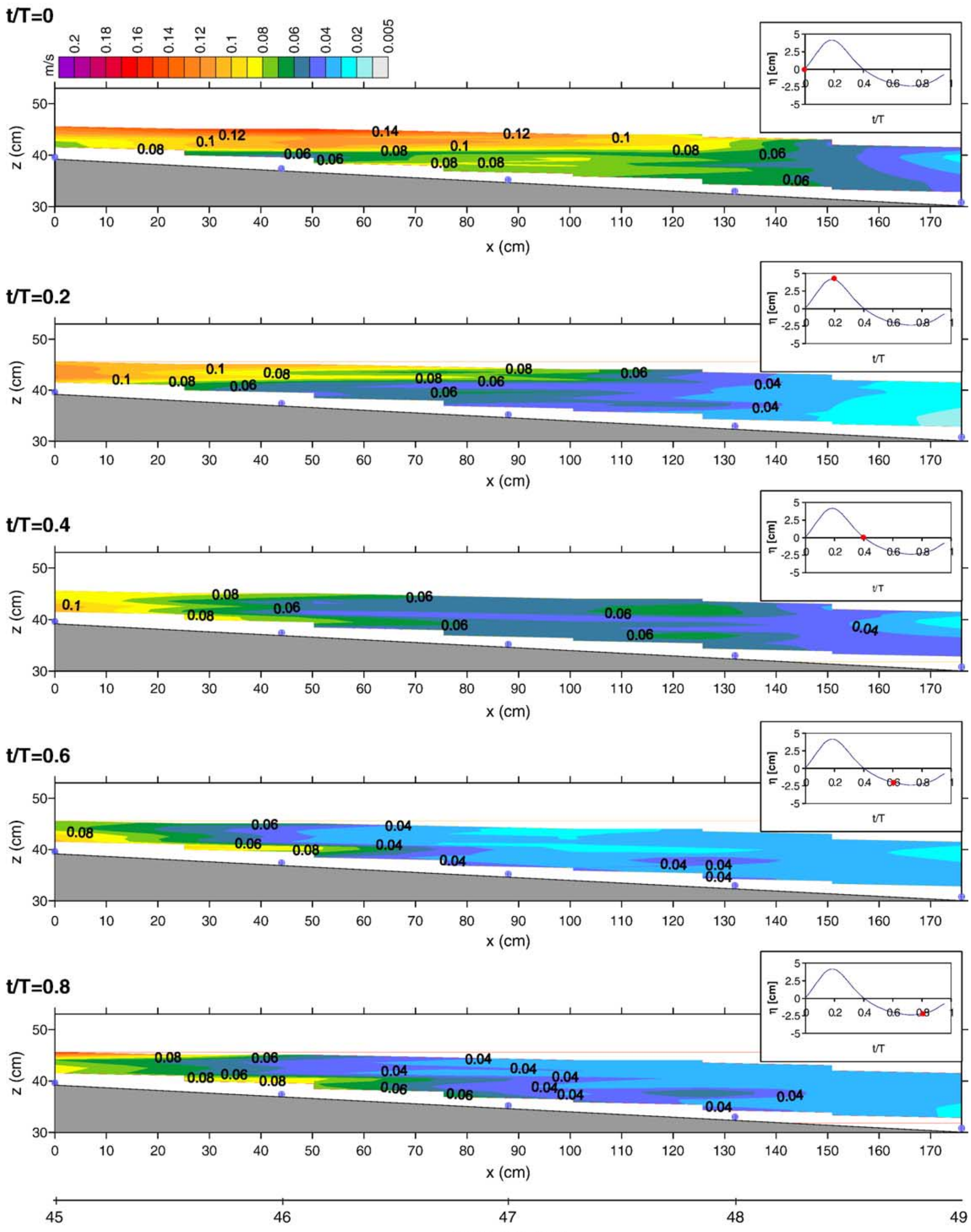

Fig. 12. Test 2–SPILLING breaking: horizontal turbulent intensities.

ward. In the case of plunging breaking, from the analysis of Fig. 9, it appears that under the wave front, both the minimum negative values of $\langle u'k' \rangle$ and $\langle w'k' \rangle$ are present. A positive peak of $\langle u'k' \rangle$ is shown near the surface, during the wave trough-crest passage. It is possible to conclude that in this case the transport of turbulent kinetic energy by turbulent velocity fluctuations is seaward and downward.

It should be pointed out that Ting and Kirby (1995, 1996) based their considerations on the aforementioned $\langle u'k' \rangle$ and $\langle w'k' \rangle$ by evaluating the diagrams of some turbulent quantities that are terms of $\langle u'k' \rangle$ and $\langle w'k' \rangle$, i.e., they indirectly derived these fluxes.

In order to demonstrate that the structures of turbulence in spilling and plunging breakers are different, a simple index is considered which links the components of the Reynolds stress tensor (Ting and Kirby, 1996). The profile of $\overline{w'^2}/\overline{u'^2}$ is shown in Fig. 10 for the spilling case, and in Fig. 11 for the plunging case.

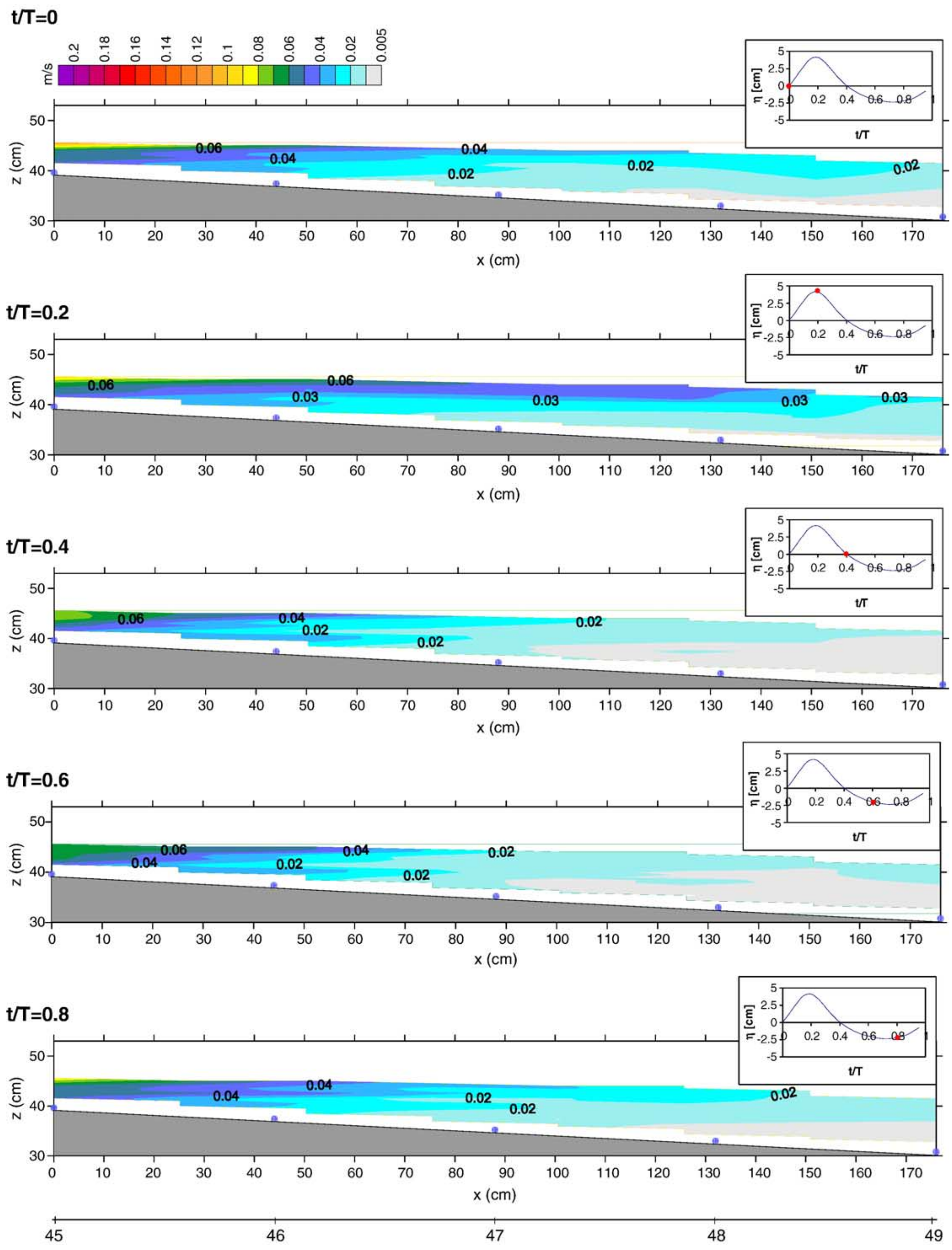

Fig. 13. Test 2 – SPILLING breaking: vertical turbulent intensities.

The results refer to both sections 47 and 48, in order to present the variation trend of the index along the surf zone. Fig. 10 shows that $\overline{w'^2}/\overline{u'^2}$ varies considerably across the surf zone. It also varies with depth, decreasing from surface to bottom with the same order of magnitude both for section 47 and section 48. Fig. 11 plots $\overline{w'^2}/\overline{u'^2}$ in the plunging breaker. The variation across the surf zone is now a bit more evident than in Fig. 10. Besides, in this case, the index decreases with distance from the surface more than in the spilling case. This aspect is probably because the turbulent motion is dominated by large eddies with large length and velocity scales, thus causing a much faster turbulent diffusion.

In the following, the trends of the phase averaged horizontal $\sqrt{\langle u'^2 \rangle}$ and vertical $\sqrt{\langle w'^2 \rangle}$ turbulent intensities in the surf zone are plotted, both for spilling (Figs. 12 and 13, respectively) and plunging case (Figs. 14 and 15, respectively). Each contour map shows the spatial distribution of the turbulent intensities at the same wave phase. Therefore, starting with spilling results

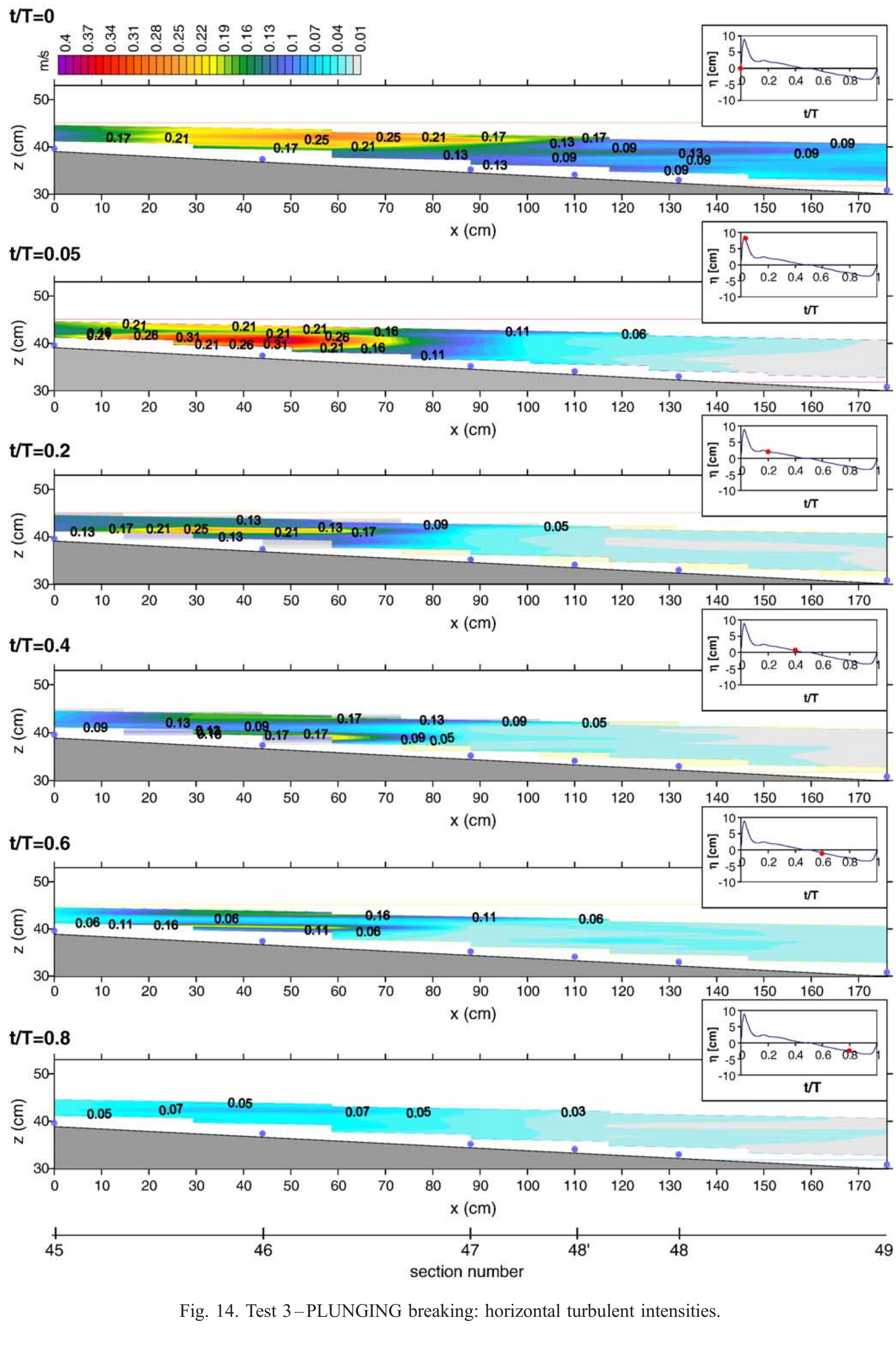

Fig. 14. Test 3 – PLUNGING breaking: horizontal turbulent intensities.

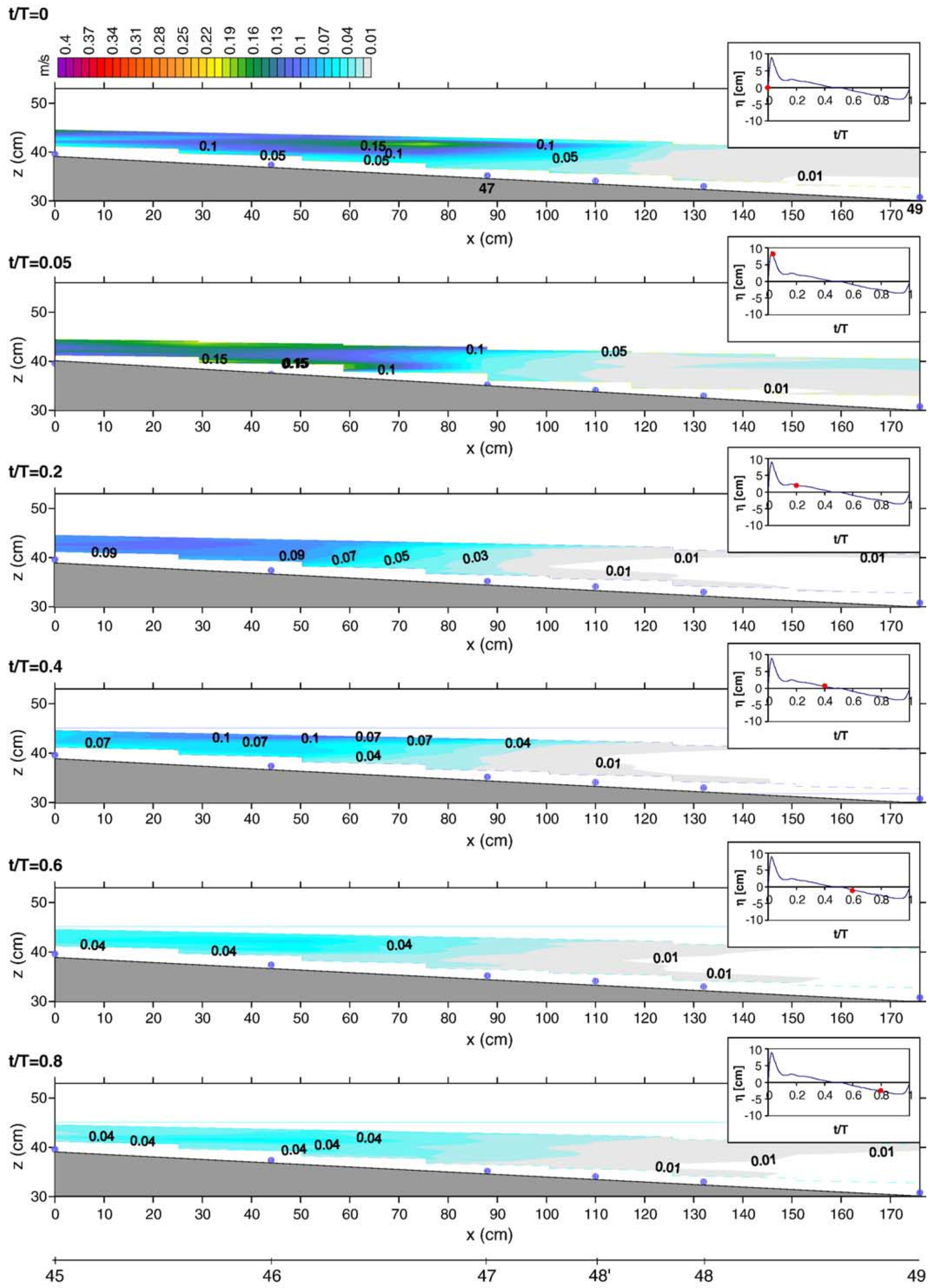

Fig. 15. Test 3 – PLUNGING breaking: vertical turbulent intensities.

(test 2), the analysis of Fig. 12 highlights that in all the investigated sections, the horizontal turbulent intensities present maximum values when the elevation becomes positive ($t/T=0$), before the crest passes, and that significant values are visible only onshore of the breaking point. Moreover, higher turbulence is localized near the surface rather than near the bottom. Under the crest ($t/T=0.2$), the horizontal turbulent intensities decrease and they still persist in the innermost sections. These values become much smaller in the successive phases, starting to increase again at $t/T=0.8$ after the trough passes. These results are expected, and as in spilling breaking, the surface roller is confined to a superficial region and precedes the crest.

Fig. 13 shows the distribution of $\sqrt{\langle w^2 \rangle}$. It can be observed that the vertical turbulent intensities are small in the spilling case if compared with the horizontal ones, and that they are quite negligible when the elevation is negative.

It is clear that both $\sqrt{\langle u^2 \rangle}$ and $\sqrt{\langle w^2 \rangle}$ are higher in plunging breaking, with respect to the spilling breaking. From Fig. 14, it is possible to observe that in the passage trough-crest ($t/T=0$) the horizontal turbulent intensities show significant values, starting from the breaking section, and they reach the maximum under the crest and immediately after the wave breaking ($t/T=0.05$). Moreover, these highest values concern a region onshore of the breaking section, spreading towards the bottom. Therefore, this distribution seems to be in accordance with the existence of the splashing jet. After the wave crest passes, $\sqrt{\langle u'^2 \rangle}$ values rapidly decrease, as can be observed at $t/T=0.2$ where it is confined near the bottom, and they reach the minimum when approaching the trough ($t/T=0.8$). Consequently, turbulence dies out between two consecutive breakers. This trend confirms Ting and Kirby's (1995) observations. An analogous behaviour can be deduced in the distribution of the vertical turbulent intensities (Fig. 15).

6. Conclusions

This experimental research deals with spilling, spilling/plunging and plunging breakers generated by three different regular waves, focusing on two aspects: the velocity and Reynolds shear stress distributions in the shoaling zone and the spreading of turbulence in the breaking region.

Regarding the first point, it was possible to directly estimate the vertical distributions of the Reynolds shear stresses $\overline{\tilde{u}\tilde{w}}$, which confirm the theoretical models of Rivero and S.-Arcilla (1995) and Deigaard and Fredsøe (1989). Also, the vertical distributions of the turbulent velocity cross-correlations $\overline{u'w'}$ were considered, observing that they are significant only close to the breaking zone.

Regarding the second point, the analysis of horizontal and vertical fluxes of turbulent kinetic energy driven by advection in the surf zone at various depths highlights that in the spilling breaker, the net sediment transport is offshore, while in the plunging breaker, it is onshore. The examination of the depth-integrated horizontal flux of turbulent kinetic energy shows that in the spilling case, it spreads away from the volume offshore of the outer zone, and it enters the volume of transition from the outer to the inner zone. In the plunging case, the depth-integrated $\langle u \rangle k$ enters the volume immediately offshore of the breaking zone, while it spreads away from the volume of breaking.

Also, the turbulent kinetic energy transport by turbulent velocity fluctuations was examined, observing that it seems essentially directed shoreward and downward in the spilling case, while it is directed seaward and downward in the plunging case. Moreover, in spilling breaking turbulence spreads slowly towards the bottom, whereas the vertical mixing is faster in the plunging breaking, due to the presence of eddies of larger scale.

Finally, the spatial distribution of the turbulent intensities was analysed, highlighting generally greater values for the plunging breaker and maximum values near the surface for the spilling case and, on the contrary, near the bottom for the plunging case.

References

Christensen, E.D., Deigaard, R., 2001. Large eddy simulation of breaking waves. Coastal Engineering 42, 53–86.

Christensen, E.D., Walstra, D.-J., Emerat, N., 2002. Vertical variation of the flow across the surf zone. Coastal Engineering 45, 169–198.

Damiani, L., Mossa, M., 1999. On turbulence in a wave field. Proc. 5th Intl. Conf. on Coastal and Port Engineering in Developing Countries. Cape Town, South Africa, pp. 25–36.

Deigaard, R., Fredsøe, J., 1989. Shear stress distribution in dissipative water waves. Coastal Engineering 13, 357–378.

De Serio, F., Mossa, M., 2003a. Experimental study on spilling and plunging breaking. Proc. Intl. Symposium on Shallow Flows, Delft, The Netherlands.

De Serio, F., Mossa, M., 2003b. Experimental study on the mechanics of regular waves. Proc. 30th IAHR Congress, Thessaloniki, Greece.

Elfrink, B., Baldock, T., 2002. Hydrodynamics and sediment transport in the swash zone: a review and perspectives. Coastal Engineering 45, 149–167.

Feng, T., Stansby, P.K., 2002. Reynolds stresses in spilling and plunging breaking waves. Proc. 28th Intl. Conf. On Coast. Eng, Wales, Cardiff, pp. 356–368.

Gudmestad, O.T., Connor, J.J., 1980. Engineering approximation to non linear deep water waves. Journal of Applied Ocean Research 8, 76–88.

Longo, S., Petti, M., Losada, I.J., 2002. Turbulence in the swash and surf zones: a review. Coastal Engineering 45, 129–147.

Okaiasu, A., Shibayama, T., Mimura, N., 1986. Velocity field under plunging waves. Proc. 20th Intl. Conf. On Coast. Eng., Taipei, Taiwan, pp. 660–674.

Pedersen, C., Deigaard, R., Sutherland, J., 1998. Measurements of the vertical correlation in turbulence under broken waves. Coastal Engineering 35, 231–249.

Petti, M., Longo, S., 2001. Turbulence experiments in the swash zone. Coastal Engineering 43, 1–24.

Rivero, F.J., S.-Arcilla, A., 1995. On vertical distribution of $\langle \tilde{u}\tilde{w} \rangle$. Costal Engineering 25, 137–152.

Rivero, F.J., S.-Arcilla, A., 1997. Discussion on the vertical distribution of $\langle \tilde{u}\tilde{w} \rangle$: reply to the comments of Z.J. You. Coastal Engineering 30, 311–315.

Stive, M.J.F., 1980. Velocity and pressure field of spilling breakers. XVII Coastal Engineering Conference, Sydney, Australia.

Stive, M.J.F., 1985. Energy dissipation in waves breaking on gentle slopes. Coastal Engineering 8, 99–127.

Svendsen, I.A., 1984. Mass flux and undertow in a surf zone. Coastal Engineering 8, 347–364.

Svendsen, I.A., 1987. Analysis of surf zone turbulence. Journal of Geophysical Research 92 (C5), 5115–5124.

Ting, F.C.K., Kirby, J.T., 1994. Observation of undertow and turbulence in a laboratory surf zone. Coastal Engineering 24, 51–80.

Ting, F.C.K., Kirby, J.T., 1995. Dynamics of surf-zone turbulence in a strong plunging breaker. Coastal Engineering 24, 177–204.

Ting, F.C.K., Kirby, J.T., 1996. Dynamics of surf-zone turbulence in a spilling breaker. Coastal Engineering 27, 305–310.

You, Z.J., 1997. Discussion on the vertical distribution of $\langle \tilde{u}\tilde{w} \rangle$ by F.J. Rivero and A.S.-Arcilla: comments. Coastal Engineering 30, 305–310.